# Tensile Strength Enhancement of Aisi 304 and Aisi 1040 Dissimilar Friction Weld Joints using Anfis Modelling

**N. Mathiazhagan, I. Rajkumar**

***Abstract*: Friction welding is a promising technique for the welding of dissimilar metals. This study deals with the welding of two different alloys, namely, AISI 304 and AISI 1040. The welding process parameters, namely, friction pressure, friction time, forging pressure, and forging time were optimized for maximum tensile strength using a response surface methodology (RSM)-based technique and an adaptive-network-based fuzzy inference system (ANFIS) model. The predicted responses obtained using the ANFIS model were more accurate compared to those obtained using the RSM. From among the four input parameters examined in the study, the frictional pressure was found to be the most influential. The ANFIS model developed in this study shows significant promise as a predictive technique that can provide reasonable estimates of tensile strength for different welding parameters.***

***Keywords* : Adaptive-network-based fuzzy inference system, Friction welding, Frictional pressure, Response surface methodology, Tensile strength.**

## I. INTRODUCTION

Friction welding (FW) is a melt-free, solid-state welding process that uses the heat generated by friction arising from the relative motion of the parts to be welded together. Friction welded joints have a remarkably high static strength and a fine-grained structure arising from the thermo-mechanical working. FW process is efficient concerning joint strength as well as energy requirements and does not require more expertise on the part of the operator. In addition, the process does not produce any emissions, fumes, or pollutants, making it environmentally friendly [1, 2]. The FW process comprises two stages, namely, heating and upsetting. The component parts with locally raised temperatures are fused together by the application of a compressive "upset" force applied laterally. In the first stage, the surfaces to be welded are kept in contact, and one of them is rotated while the other is held stationary against the rotating part with the application of a particular pressure. The second stage commences once the required temperature is attained. The rotation is stopped instantaneously while the pressure is increased sharply.

**Revised Manuscript Received on October 15, 2019**

**N.Mathiazhagan***, Professor, Department of Mechanical Engineering, Meenakshi Ramaswamy Engineering College, Ariyalur, Tamil Nadu, India. . Email: nallmathi67@gmail.com

**I.Rajkumar**, Assistant Professor, Department of Mechanical Engineering, C. Abdul Hakeem College of Engineering & Technology, Melvisharam, Tamilnadu, India. Email: irksami@gmail.com.

This force causes the plastic deformation of the surfaces in contact and contrast with traditional fusion welding techniques; the parts are joined together by forging rather than by the melting or fusion of the materials [3, 4]. FW is of particular use in the joining of difficult-to-weld or low-melting materials. It can also be used to replace forging or casting assembly. Dissimilar welding is another important area of application, which is often required in the automotive, marine, aerospace, and oil industries [5]. Joining dissimilar metals by welding is challenging due to the differences in their crystal structure as well as chemical and mechanical properties. Conventional fusion welding techniques give rise to the formation of secondary phases in the welds. FW, however, can produce higher strength welds in dissimilar metals than other favorite welding techniques. Friction welds are void free and airtight, with both metals present across the entire weld cross section and only minimal extent of heat affected zone [6].

Dissimilar metals may need to be joined together to obtain particular material property profiles, utilize scarce material effectively, or reduce cost [7, 8]. AISI 304 is a commonly used grade of austenitic stainless steel. It has excellent corrosion resistance and can be safely used in various corrosive environments. AISI 1040 has high carbon content and can be heat treated to obtain high hardness. This study pertains to the FW of AISI 304 and AISI 1040 to form dissimilar-metal joints. The optimal choice of welding parameters have a significant role in the effectiveness of the joining process. several authors have reported that the optimization of FW parameters, such as friction pressure, friction time, forging pressure, and forging time, is effective in obtaining maximum tensile strengths in dissimilar-metal joints of austenitic stainless steel and medium carbon steel [9 - 11]. Prasanthi et al. studied the joining of dissimilar materials, namely, mild steel and titanium and optimized several process parameters to obtain defect-free interfaces. The authors found that FW followed by appropriate heat treatment generated weld interfaces that were of the required quality [12].

The microstructural properties of solid-state friction welded Titanium alloy samples were prepared using selective laser melting (SLM) and the authors concluded that FW was effective for welding SLM parts and can contribute to improving their ductility [13]. In a relatively early study, Paventhan et al. proposed an empirical relationship that relates the tensile strength of FW joints of AISI 304 and AA 6082 aluminum alloy. Response surface methodology (RSM) was used to optimize the process parameters. Further studies dealt with the optimization of process parameters for the maximum tensile strength of AISI 304 and AISI 1040 steel [14, 15]. In both these studies, the parameters considered were the friction pressure, forging pressure, friction time, and forging time. An empirical relationship was developed to quantify the effect of process parameters on the obtained tensile strength of titanium tubes fabricated by FW. In a similar work the microstructural characteristics and ultimate tensile strength of similar titanium tubes were studied in detail using extensive experimentation [16, 17]. Meisnar et al. investigated the FW dissimilar materials Ti-6Al-4V and AA6082 for space applications. The authors state that even as thorough optimization of welding parameters have resulted in high-quality welds, the complexities inherent in the FW process may yet cause brittle intermetallic compounds to form at the weld interface [18].

Selvamani and Palanikumar [19] used ANOVA methods to establish empirical relationships between the process parameter combinations and process outcomes such as the tensile strengths and percentage of elongation of the welded joints. Senkov et al. examined the process parameters of inertia friction welding and related them to welding process outcomes, especially from the point of view of the flywheel energy [20]. Furthermore, the experimental studies on FW of UNS S31803 DSS joints and the results of which were used to validate a nonlinear three-dimensional finite element model. The validated model could potentially be used for performing further simulations and predictive studies [21]. Balta et al. studied the longevity and structural integrity of steel tube/forging joints prepared using continuous drive friction welding (CFDW). RSM was used to relate the welding parameters, namely, friction pressure, friction time, forging pressure and forging time, and the mechanical properties of the welded joint. A desirability function was established for determining the optimal parameter values, and the use of petal test for FW optimization was pioneered [22].

The FW of dissimilar, metal-reinforced polymer materials was studied by Kumar et al., who subsequently used an RSM-based statistical method for improving the weldability [23]. Artificial neural networks (ANNs) are brain-inspired computing systems that can learn new behavior using examples and used for the variety of problems. Mathematical modelling of friction surface response is possible by artificial neural networks (ANNs). Winiezenko developed an empirical relationship using hybrid RSM and genetic algorithm (GA) for dissimilar friction welding of AISI 1020 and ASTM 536 iron. The model optimized the input parameters to maximize the tensile strength of the joints [24].

ANNs attempts to correlate between FW process parameters and mechanical properties by linking them. Hussain et al. predicted the tensile and shear strength of friction surfaced tool steel deposit by feed forward neural network (FFNN) consisting of three layers [25]. With regard to multi-objective optimization, Ajith et al. (2017a) used a multi-layer perceptron neural network in conjunction with the particle swarm optimization method to model the FW of a DSS sample and optimize the welding parameters to maximize the tensile strength and microhardness of the welded sample. The process parameters chosen for optimization are the friction pressure, upset pressure, welding speed, and burn-off length. In another study (Ajith et al., 2017b), the same problem was addressed using the RSM in conjunction with a genetic algorithm [26, 27].

It is observed that modeling of the FW process is an iterative technique for predicting the responses. Starting with the mathematical modeling, attempts have been made to apply various available techniques for forecasting the predicted experiment values and outcomes. However, as FW is a relatively advanced technology, few attempts have been made in this regard [28 - 30]. An adaptive neuro-fuzzy inference system or adaptive-network-based fuzzy inference system (ANFIS) is a class of neural network that is based on the Takagi–Sugeno fuzzy inference system and integrates both neural network and fuzzy logic principles [31 - 33]. Yulius Eka Agung Seputra and Bambang Soegijono employed ANFIS simulation models to predict the experimental and computational design relationship of aluminium matrix composite (AMC) variables [34]. Ansari et al. optimized plunging phase of friction stir welding (FSW) process using smoothed particle hydrodynamics (SPH) method in ABAQUS software and concluded that SPH is preferred for validating plunging force and stress, strain distribution [35]. Based on both human knowledge and stipulated input-output data pairs, ANFIS proposed in this investigation constructs an input-output mapping. Weld parameters and the mechanical properties relationship are developed via ANFIS and RSM. It is attempted to optimize the FW process parameters to obtain the maximum tensile strength in dissimilar joints of AISI 304 austenitic stainless steel and AISI 1040 grade medium carbon steel using the RSM and ANFIS. The study also aims to identify a useful tool for the analysis and prediction of FW process parameters, develop an empirical relationship between the process parameters and the tensile property of the dissimilar joints, and to identify the influential parameter in the FW process.

## II. EXPERIMENTATION

The dissimilar parent materials considered for this investigation are austenitic stainless steel (ASS) AISI 304 and medium carbon steel (MCS) AISI 1040, whose chemical composition (wt %) are given in Table 1.The parameter levels of the FW parameters chosen from preliminary welding trials were categorized as low, medium, and high. Table 1a presents the upper and lower limits as well as the different levels of process parameters used in the study. Tensile tests were conducted on welded samples, machined as per ASTM E8 / E8M-16a (2016) standards [36], using the experimental set-up shown in Fig. 1, with cylindrical tensile test and notched tensile test specimens of the type shown in Fig. 2(a) and 2(b) respectively.


**Fig.1. Experimental set-up**

**Table-1: Chemical composition (wt%) of parent materials**

| Material | C | P | S | Mn | Si | Ni | Cr | Fe |
|---|---|---|---|---|---|---|---|---|
| ASS (AISI 304) | 0.046 | 0.044 | 0.006 | 1.20 | 0.44 | 8.17 | 18.33 | Bal |
| MCS (AISI 1040) | 0.38 | 0.04 | 0.05 | 0.75 | 0.20 | - | - | Bal |

**Table-1a : Levels of Process parameters**

| Sl.No | Factor | Unit | Notation | Levels | | | | |
|---|---|---|---|---|---|---|---|---|
| | | | | -2 | -1 | 0 | 1 | 2 |
| 1 | Friction pressure | MPa | A | 50 | 70 | 90 | 110 | 130 |
| 2 | Friction time | Seconds | B | 2 | 4 | 6 | 8 | 10 |
| 3 | Forging pressure | MPa | C | 50 | 70 | 90 | 110 | 130 |
| 4 | Forging time | Seconds | D | 2 | 4 | 6 | 8 | 10 |

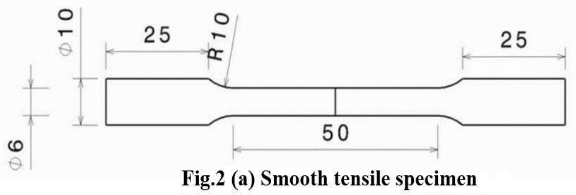


Fig.2 (a) Smooth tensile specimen

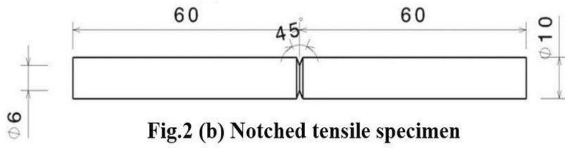


Fig.2 (b) Notched tensile specimen

**Fig.2. Dimensions of specimen prepared for tensile test**

RSM is a statistical approach that can be used to determine the relationship between two sets of variables – the first set being the input and the second being the responses. A sequence of designed experiments that use different combinations of parameter values and obtains the corresponding set of responses is used for this purpose [37]. In this study, four factors at five levels are considered to establish an empirical relationship between the critical process parameters. The parameter levels pertaining to the designed experiments are shown in Table 2. The process parameters and the measured tensile strength from each run of the experiment are provided in Table 3. Figs. 3(a)-(d) show samples of the test specimens before and after they are subjected to tensile tests.

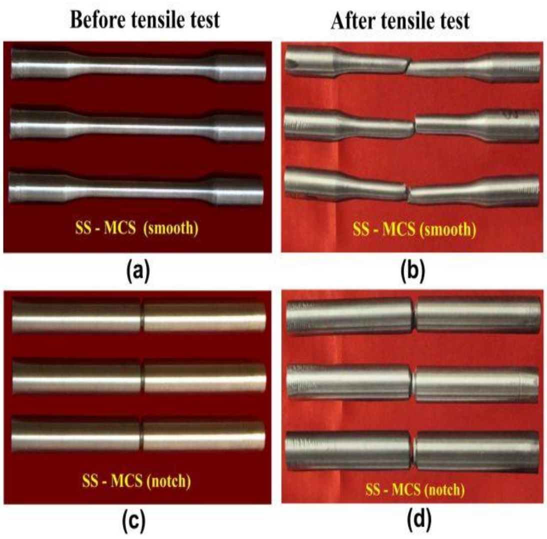


**Fig.3. Photographs of tensile test specimens**

**Table-2 : Experimental Design**

| Sl. No. | A | B | C | D |
|---|---|---|---|---|
| **1.** | 0.00 | -2.00 | 0.00 | 0.00 |
| **2.** | -1.00 | -1.00 | -1.00 | 1.00 |
| **3.** | 1.00 | -1.00 | 1.00 | 1.00 |
| **4.** | -1.00 | 1.00 | -1.00 | -1.00 |
| **5.** | -1.00 | -1.00 | 1.00 | 1.00 |
| **6.** | 0.00 | 0.00 | 0.00 | 0.00 |
| **7.** | 0.00 | 0.00 | 0.00 | 0.00 |
| **8.** | -2.00 | 0.00 | 0.00 | 0.00 |
| **9.** | 1.00 | -1.00 | -1.00 | -1.00 |
| **10.** | -1.00 | -1.00 | -1.00 | -1.00 |
| **11.** | -1.00 | -1.00 | 1.00 | -1.00 |
| **12.** | 0.00 | 0.00 | -2.00 | 0.00 |
| **13.** | 1.00 | -1.00 | -1.00 | 1.00 |
| **14.** | 1.00 | 1.00 | 1.00 | -1.00 |
| **15.** | -1.00 | 1.00 | -1.00 | 1.00 |
| **16.** | 0.00 | 0.00 | 2.00 | 0.00 |
| **17.** | 0.00 | 2.00 | 0.00 | 0.00 |
| **18.** | 0.00 | 0.00 | 0.00 | 0.00 |
| **19.** | 1.00 | 1.00 | -1.00 | -1.00 |
| **20.** | 2.00 | 0.00 | 0.00 | 0.00 |
| **21.** | 0.00 | 0.00 | 0.00 | 0.00 |
| **22.** | -1.00 | 1.00 | 1.00 | -1.00 |
| **23.** | -1.00 | 1.00 | 1.00 | 1.00 |
| **24.** | 1.00 | -1.00 | 1.00 | -1.00 |
| **25.** | 1.00 | 1.00 | 1.00 | 1.00 |
| **26.** | 0.00 | 0.00 | 0.00 | 0.00 |
| **27.** | 1.00 | 1.00 | -1.00 | 1.00 |
| **28.** | 0.00 | 0.00 | 0.00 | -2.00 |
| **29.** | 0.00 | 0.00 | 0.00 | 0.00 |
| **30.** | 0.00 | 0.00 | 0.00 | 2.00 |

**Table-3 : Process parameters and their corresponding response**

| Sl. No. | A | B | C | D | E |
|---|---|---|---|---|---|
| 1. | 90 | 2 | 90 | 6 | 422 |
| 2. | 70 | 4 | 70 | 8 | 450 |
| 3. | 110 | 4 | 110 | 8 | 469 |
| 4. | 70 | 8 | 70 | 4 | 483 |
| 5. | 70 | 4 | 110 | 8 | 495 |
| 6. | 90 | 6 | 90 | 6 | 535 |
| 7. | 90 | 6 | 90 | 6 | 540 |
| 8. | 50 | 6 | 90 | 6 | 452 |
| 9. | 110 | 4 | 70 | 4 | 488 |
| 10. | 70 | 4 | 70 | 4 | 469 |
| 11. | 70 | 4 | 110 | 4 | 461 |
| 12. | 90 | 6 | 50 | 6 | 501 |
| 13. | 110 | 4 | 70 | 8 | 461 |
| 14. | 110 | 8 | 110 | 4 | 486 |
| 15. | 70 | 8 | 70 | 8 | 465 |
| 16. | 90 | 6 | 130 | 6 | 514 |
| 17. | 90 | 10 | 90 | 6 | 452 |
| 18. | 90 | 6 | 90 | 6 | 551 |
| 19. | 110 | 8 | 70 | 4 | 513 |
| 20. | 130 | 6 | 90 | 6 | 475 |
| 21. | 90 | 6 | 90 | 6 | 541 |
| 22. | 70 | 8 | 110 | 4 | 470 |
| 23. | 70 | 8 | 110 | 8 | 499 |
| 24. | 110 | 4 | 110 | 4 | 460 |
| 25. | 110 | 8 | 110 | 8 | 493 |
| 26. | 90 | 6 | 90 | 6 | 546 |
| 27. | 110 | 8 | 70 | 8 | 489 |
| 28. | 90 | 6 | 90 | 2 | 514 |
| 29. | 90 | 6 | 90 | 6 | 539 |
| 30. | 90 | 6 | 90 | 10 | 515 |

**A = Friction Pressure B = Friction Time C = Forging Pressure D = Forging Time E = Tensile Strength**

The empirical relationship between the process parameters and the tensile property of the welded joints were developed using the RSM. Based on the experimental runs, the predicted tensile strength of the specimens have been obtained as:

$$E = -410.219 + 10.670A + 78.615B + 4.182C + 7.073D$$
$$-0.50A^2 - 6064B^2 - 0.023C^2 - 1.82D^2 + 0.095AB$$
$$-0.016AC - 0.095AD - 0.030BC - 0.047BD + 0.261CD \quad (1)$$

The predicted values of the tensile strength obtained from the RSM-generated correlation is listed in Table 4.

**Table-4 : Predicted response using RSM**

| Sl. No. | A | B | C | D | E | F |
|---|---|---|---|---|---|---|
| 1. | 90 | 2 | 90 | 6 | 422 | 413.829 |
| 2. | 70 | 4 | 70 | 8 | 450 | 450.917 |
| 3. | 110 | 4 | 110 | 8 | 469 | 467.717 |
| 4. | 70 | 8 | 70 | 4 | 483 | 476.293 |
| 5. | 70 | 4 | 110 | 8 | 495 | 486.517 |
| 6. | 90 | 6 | 90 | 6 | 535 | 537.313 |
| 7. | 90 | 6 | 90 | 6 | 540 | 537.313 |
| 8. | 50 | 6 | 90 | 6 | 452 | 448.113 |
| 9. | 110 | 4 | 70 | 4 | 488 | 486.257 |
| 10. | 70 | 4 | 70 | 4 | 469 | 464.257 |
| 11. | 70 | 4 | 110 | 4 | 461 | 458.097 |
| 12. | 90 | 6 | 50 | 6 | 501 | 500.993 |
| 13. | 110 | 4 | 70 | 8 | 461 | 457.717 |
| 14. | 110 | 8 | 110 | 4 | 486 | 476.933 |
| 15. | 70 | 8 | 70 | 8 | 465 | 462.201 |
| 16. | 90 | 6 | 130 | 6 | 514 | 500.033 |
| 17. | 90 | 10 | 90 | 6 | 452 | 447.549 |
| 18. | 90 | 6 | 90 | 6 | 551 | 537.313 |
| 19. | 110 | 8 | 70 | 4 | 513 | 513.493 |
| 20. | 130 | 6 | 90 | 6 | 475 | 466.513 |
| 21. | 90 | 6 | 90 | 6 | 541 | 537.313 |
| 22. | 70 | 8 | 110 | 4 | 470 | 465.333 |
| 23. | 70 | 8 | 110 | 8 | 499 | 493.001 |
| 24. | 110 | 4 | 110 | 4 | 460 | 454.497 |
| 25. | 110 | 8 | 110 | 8 | 493 | 489.401 |
| 26. | 90 | 6 | 90 | 6 | 546 | 537.313 |
| 27. | 110 | 8 | 70 | 8 | 489 | 484.201 |
| 28. | 90 | 6 | 90 | 2 | 514 | 508.629 |
| 29. | 90 | 6 | 90 | 6 | 539 | 537.313 |
| 30. | 90 | 6 | 90 | 10 | 515 | 507.757 |

**A = Friction Pressure B = Friction Time C = Forging Pressure D = Forging Time E = Tensile Strength F - Predicted Tensile Strength**

It can be observed from the tabulated data that these predicted tensile strength values differ slightly from the measured values. The contour plots shown in Figs. 4, 5, and 6 visualize the relationships between the tensile strength and the process parameters.

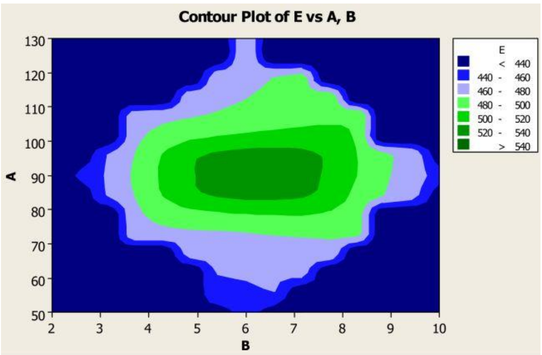


**Fig.4. Contour plot of tensile strength for friction pressure and friction time.**

Fig. 4 plots the variation of tensile strength with different values of friction pressure and friction time. It can be observed from the plot that moderate values of both friction pressure and friction time give the highest tensile strength values. However, the effect of friction pressure is more pronounced.

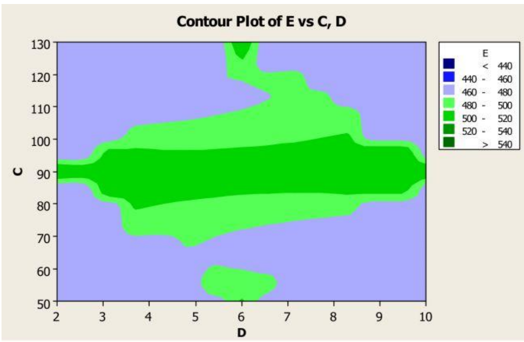

**Fig.5. Contour plot of tensile strength for forging pressure and forging time**

Fig. 5 represents the variation of tensile strength with forging pressure and forging time. The maximum tensile strength values seem clustered near moderate values of forging pressure while forging time does not appear to have a significant effect. Fig. 6 represents the variation of tensile strength with friction pressure and forging pressure. For moderate values of friction pressure and forging pressure, the tensile strength values are maximized, as can be seen from the counterplots.

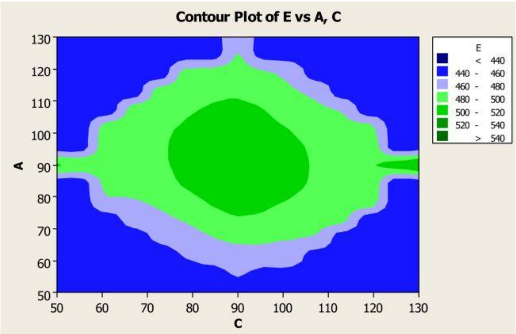


**Fig.6. Contour plot of tensile strength for friction pressure and forging pressure**

## III. OPTIMIZATION USING ANFIS

The necessary steps in a fuzzy logic-based inference system are the mapping of input characteristics to chosen input membership functions, which are further mapped to a set of rules. These rules are then mapped to the output characteristics, which in turn, are mapped to output membership functions and subsequently, to a single-valued output or decision. ANFIS uses the principles of both ANNs and fuzzy logic and is a robust framework that incorporates the best characteristics of both the methods. ANFIS use either a back propagation algorithm or a combination of such an algorithm and a least-squares method that allows the neural network to be trained using the very data that it models [38]. This study uses the MATLAB Fuzzy Logic Toolbox for modeling the experimental data and optimizing the process parameters. The choice of the membership function is usually performed by the software to allow for the best correlation of the input and output data. Fig. 7 shows the parameters of the proposed ANFIS model as defined using the graphical user interface (GUI) of the software.

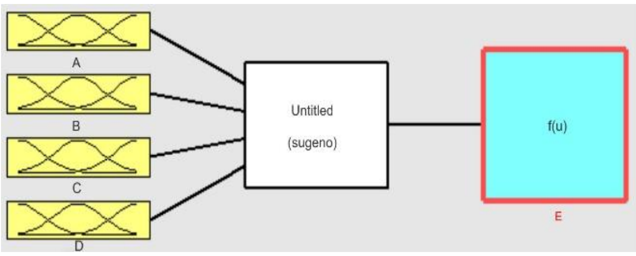


**Fig.7. Proposed ANFIS model**

The FIS type selected is Sugeno, which is based on the Takagi–Sugeno-Kang method. In this method, the membership functions related to the output parameters are either linear or constant.

As per a typical Sugeno rule, if the input parameters are represented by x and y, the output will be of the form:

$$z = ax + by + c \tag{2}$$

where a,b,and c are constants.

The firing strength of the rule, $w_i$ is used to weight the output level $z_i$. For example, the firing strength $w_i$ for an AND rule with inputs $x$ and $y$ is given by

$$w_i = AndMethod\,(F_1(x), F_2(y)) \tag{3}$$

where $F_1$ and $F_2$ represent the membership functions for the inputs $x$ and $y$.The final output obtained from the system is the weighted average of the outputs obtained from all the N rules, given by

$$f(u) = \frac{\sum_{i=1}^{N} w_i z_i}{\sum_{i=1}^{N} w_i} \tag{4}$$

The welding parameters denoted as A, B, C, and D are the inputs to the model, and the output is denoted as $f(u)$. Fig. 8 shows the input data that is provided as input to the model. These 30 data pairs are obtained from the experiments, as tabulated in Table 2, corresponding to each of the 30 runs of the experiment.

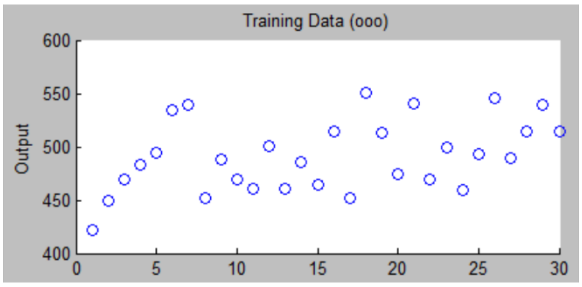


**Fig.8. Loading the data**

A linear membership function is selected from the set of membership functions available in the fuzzy logic toolbox. The symmetric Gaussian curve membership function chosen in this study is represented by

$$f(x;\sigma,c) = e^{\frac{-(x-c)^2}{2\sigma^2}} \tag{5}$$

where σ and c are parameters defined by the software.

Three separate membership functions of this type are assigned for each input. The structure of the proposed ANFIS model is thus summarized in Fig.9 which shows the successive mappings until a single output is obtained from the four input variables. The training data used for simulation generates error as represented by Fig.10. The predicted responses obtained from the ANFIS model for each set of parameter values are summarized in Table 5.

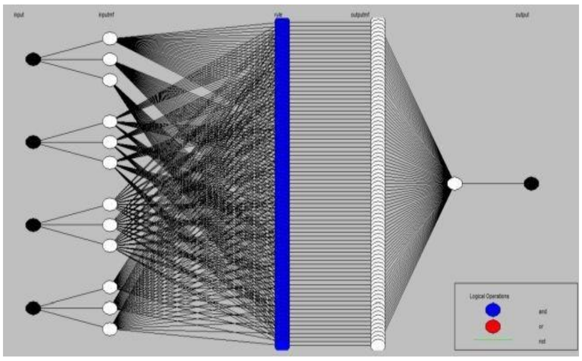

**Fig.9. Structure of the proposed ANFIS model**

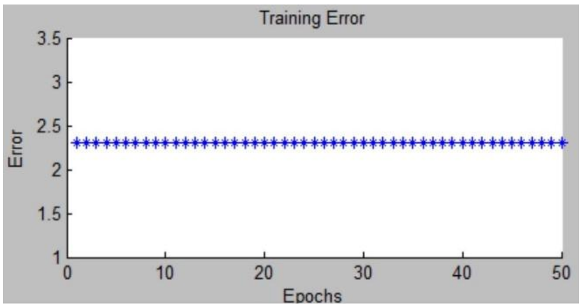


**Fig.10. Plotting of training error**

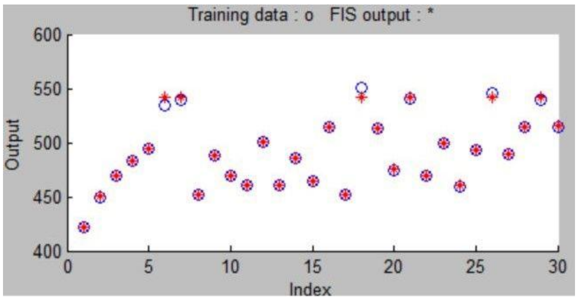


**Fig.11. Plotting of actual and predicted responses**

**Table-5 : Predicted response using ANFIS**

| Sl. No. | A | B | C | D | E | F |
|---|---|---|---|---|---|---|
| 1. | 90 | 2 | 90 | 6 | 422 | 422 |
| 2. | 70 | 4 | 70 | 8 | 450 | 450 |
| 3. | 110 | 4 | 110 | 8 | 469 | 469 |
| 4. | 70 | 8 | 70 | 4 | 483 | 483 |
| 5. | 70 | 4 | 110 | 8 | 495 | 495 |
| 6. | 90 | 6 | 90 | 6 | 535 | 542 |
| 7. | 90 | 6 | 90 | 6 | 540 | 542 |
| 8. | 50 | 6 | 90 | 6 | 452 | 452 |
| 9. | 110 | 4 | 70 | 4 | 488 | 488 |
| 10. | 70 | 4 | 70 | 4 | 469 | 469 |
| 11. | 70 | 4 | 110 | 4 | 461 | 461 |
| 12. | 90 | 6 | 50 | 6 | 501 | 501 |
| 13. | 110 | 4 | 70 | 8 | 461 | 461 |
| 14. | 110 | 8 | 110 | 4 | 486 | 486 |
| 15. | 70 | 8 | 70 | 8 | 465 | 465 |
| 16. | 90 | 6 | 130 | 6 | 514 | 514 |
| 17. | 90 | 10 | 90 | 6 | 452 | 452 |
| 18. | 90 | 6 | 90 | 6 | 551 | 542 |
| 19. | 110 | 8 | 70 | 4 | 513 | 513 |
| 20. | 130 | 6 | 90 | 6 | 475 | 475 |
| 21. | 90 | 6 | 90 | 6 | 541 | 542 |
| 22. | 70 | 8 | 110 | 4 | 470 | 470 |
| 23. | 70 | 8 | 110 | 8 | 499 | 499 |
| 24. | 110 | 4 | 110 | 4 | 460 | 460 |
| 25. | 110 | 8 | 110 | 8 | 493 | 493 |
| 26. | 90 | 6 | 90 | 6 | 546 | 542 |
| 27. | 110 | 8 | 70 | 8 | 489 | 489 |
| 28. | 90 | 6 | 90 | 2 | 514 | 514 |
| 29. | 90 | 6 | 90 | 6 | 539 | 542 |
| 30. | 90 | 6 | 90 | 10 | 515 | 515 |

**A = Friction Pressure B = Friction Time C = Forging Pressure D = Forging Time E = Tensile Strength F - Predicted Tensile Strength**

The comparison of the predicted responses with the actual measured responses is illustrated in Fig. 11.

It can be observed that in the ANFIS model, the obtained responses vary only marginally from the actual measured responses, indicating the acceptability of the model. The applied rules and output obtained for a particular combination of input values are illustrated in Fig. 12. It must be noted that similar rule combinations are applied for data from each of the 30 runs.

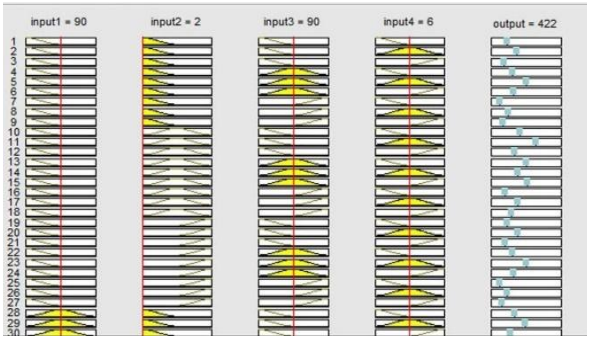


**Fig.12. Rule viewer of the proposed ANFIS model**

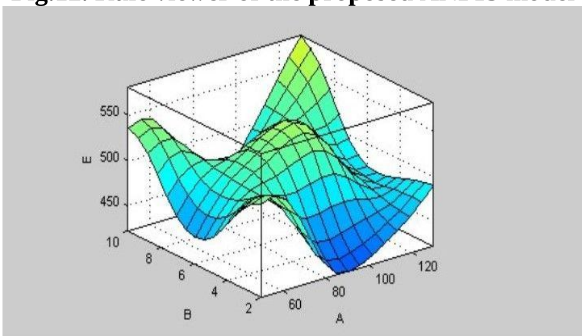

**Fig.13. Surface viewer of the tensile strength for friction pressure and friction time**

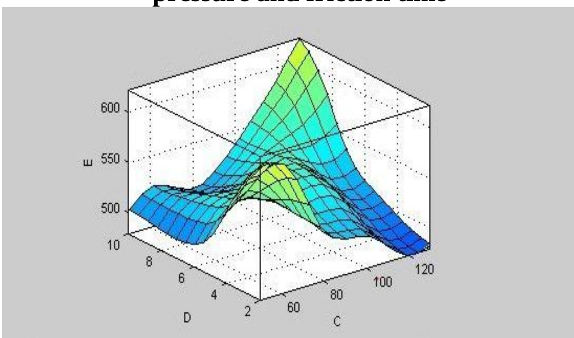

**Fig.14. Surface viewer of the tensile strength for forging pressure and forging time**

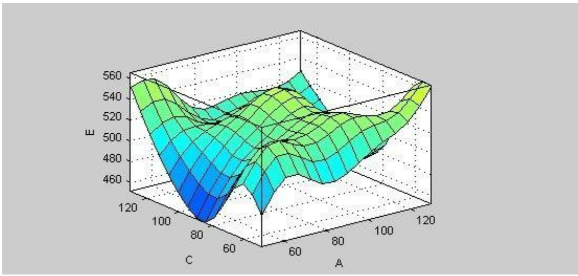

**Fig.15. Surface viewer of the tensile strength for friction pressure and forging pressure**

Figs. 13, 14, and 15 show the surface plots that elucidate the influence of friction pressure and friction time, forging pressure and forging time, and friction pressure and forging pressure, respectively, on the tensile strength of the specimen. The conclusions that can be drawn from these

Retrieval Number: A9342109119/2019©BEIESP
DOI: 10.35940/ijeat.A9342.109119



Published By:
Blue Eyes Intelligence Engineering
& Sciences Publication

surface plots are analogous to those obtained from the RSM contour plots in Figures. 4, 5, and 6.

## IV. CONCLUSIONS

In this study, the FW process parameters for the welding of dissimilar alloys, namely, AISI 304 and AISI 1040, were optimized using an RSM-based technique and ANFIS method to obtain the maxi-mum tensile strength of the welded joint. The predicted responses obtained using the ANFIS model were more accurate compared to those obtained us-ing the RSM. From among the four input parameters examined in the study, the frictional pressure was found to be the most influential. When repetitive runs using the same parameter values were conducted, the RSM-based technique predicted different tensile strength values for each of the cases while the developed ANFIS model generated the same output values for each of these same runs. The ANFIS model developed in this study shows significant promise as a predictive technique that can provide reasonable estimates of tensile strength for different welding parameters.

## ACKNOWLEDGMENT

The authors extend their sincere thanks to Dr. T.Senthil kumar, Department of Mechanical Engineering, Anna University - BIT Campus, Tiruchirappalli, Tamil Nadu for the encouragement and guidance. The authors are thankful to the Center for Materials Joining & Research (CEMAJOR), Department of Manufacturing Engineering, Annamalai University, Chidambaram for the support to carry out the experimentation.

## REFERENCES

1. A. Służalec, "Thermal effects in friction welding," *Intl. J. of Mech. Sci*, vol. 32 (6), 1990, pp. 467–478.
2. E. P. Alves, F Piorino Neto and C.Y. An, "Welding of AA1050 aluminum with AISI 304 stainless steel by rotary friction welding process," *J. Aerosp. Tech. and Mgt*, vol.2(3), 2010, pp. 301–306.
3. M. Maalekian, E. Kozeschnik, H.P. Brantner and H. Cerjak, "Comparative analysis of heat generation in friction welding of steel bars," *Acta Mater.*, vol. 56 (12), 2008, pp. 2843–2855.
4. A. Dawood, S. Butt, G. Hussain, M. Siddiqui, A. Maqsood and Zhang F, "Thermal model of rotary friction welding for similar and dissimilar metals," *Metals*, , vol.7(6), 2017, pp. 224.
5. M. Aritoshi, K. Okita, "Friction welding of dissimilar metals," *Welding Inter.*, vol. 17(4), 2003, pp. 271–275.
6. Klas Weman, "*Pressure welding methods,"* in: Welding Processes Handbook , Second ed., Woodhead Publishing Series in Welding and Other Joining Technologies, 2012, pp.119-132.
7. Sare Celik, Dincer Dinc, Ramazan Yaman, Irfan Ay, "An investigation on weldability of AISI 304 and AISI 1040 Steels on friction welding," *Practical Metallography*, vol. 47(4), 2010, pp.188-205.
8. P. Sathiya, S. Aravindan, A.N. Haq and K. Paneerselvam, "Optimization of friction welding parameters using evolutionary computational techniques," *Journal of Materials Processing Technology*, vol. 209(5), 2009, pp. 2576–2584.
9. H. Mümin Sahin, H. Erol Akata, "An experimental study on friction welding of medium carbon and austenitic stainless steel components,"
10. *Industrial Lubrication and Tribology*, vol. 56 (2), 2004, pp. 122 – 129.
11. N.R.J. Hynes and P.S. Velu, "Microstructural and mechanical properties on friction welding of dissimilar metals used in motor vehicles," *Mat. Res. Exp*, vol.5(2), 2018, pp. 026521.
12. X. Liu, S. Lan and J. Ni, "Analysis of process parameters effects on friction stir welding of dissimilar aluminum alloy to advanced high strength steel," *Mat. & Des.* Vol. 59, 2014, pp. 50–62.
13. T.N Prasanthi, C. Sudha, S. Saroja, N. Naveen Kumar and G.D. JanakiRam, "Friction welding of mild steel and titanium: optimization of process parameters and evolution of interface microstructure," *Mat. & Des.* Vol.88, 2015, pp. 58-68.
14. K.G. Prashanth, R. Damodaram, T. Maity, P. Wang and J. Eckert, "Friction welding of selective laser melted Ti6Al4V parts," *Mat. Sci. and Eng : A*, vol. 704, 2017, pp. 66-71.
15. R. Paventhan, P.R. Lakshminarayanan and V. Balasubramanian, "Prediction and optimization of friction welding parameters for joining aluminium alloy and stainless steel," *Trans. Nonfer. Met. Soc. Chi*, vol.21 (7), 2011, pp.1480-1485.
16. R. Paventhan, P.R. Lakshminarayanan and V. Balasubramanian, "Optimization of friction welding process parameters for joining carbon steel and stainless steel," *J. Iron and Ste. Res. Inter.*, vol.19 (1), 2012, pp. 66-71.
17. R. Palanivel, R.F. Laubscher and I. Dinaharan, "An investigation into the effect of friction welding parameters on the tensile strength of titanium tubes by utilizing an empirical relationship," *Meas*, vol. 098, 2017, pp. 77-91.
18. R. Palanivel, I. Dinaharan and R.F. Laubscher. "Assessment of microstructure and tensile behavior of continuous drive friction welded titanium tubes," *Mat. Sci. and Eng.: A*, vol. 687, 2017, pp. 249-258.
19. M. Meisnar, S. Baker, J.M. Bennett, A. Bernad, A. Mostafa S. Resch, N. Fernandes and A. Norman, "Microstructural characterization of rotary friction welded AA6082 and Ti-6Al-4V dissimilar joints," *Mat. & Des.*, vol. 132, 2017, pp.188-197.
20. S.T. Selvamani and K. Palanikumar, "Optimizing the friction welding parameters to attain maximum tensile strength in AISI 1035 grade carbon steel rods," *Meas*, vol.53, 2014, pp.10-21.
21. O.N. Senkov, D.W. Mahaffey and S.L. Semiatin, "Effect of process parameters on process efficiency and inertia friction welding behavior of the superalloys LSHR and Mar-M247," *J. Mat. Proc. Tech.*, vol. 250, 2017, pp.156-168.
22. M. Mohammed Asif, Shrikrishana, Kulkarni Anup and P. Sathiya, "Finite element modeling and characterization of friction welding on UNS S31803 duplex stainless steel joints," *Eng. Sci and Tech*, vol. 18(4), 2015, pp.704-712.
23. Balta Berna, A. Armagan Arici, Muharrem Yilmaz, "Optimization of process parameters for friction weld steel tube to forging joints," *Mat. & Des.*, vol.103, 2016, pp. 209-222.
24. R. Kumar, M. Balasubramanian, "Application of response surface methodology to optimize process parameters in friction welding of Ti–6Al–4V and SS304L rods," *Trans. Nonf. Met. Soc Chi.*, vol. 25 (11), 2015, pp. 3625-3633.
25. R. Winiczenko, "Effect of friction welding parameters on the tensile strength and microstructural properties of dissimilar AISI 1020-ASTM A536 joints," *Int. J. Adv.Manuf. Tech*, vol.84, 2016, pp. 941-955.
26. M. Manzoor Hussain, V. Pitchi Raju, J. Kandasamy, D. Govardhan, "Prediction of tensile and shear strength of friction surfaced tool steel deposit by using artificial neural networks," *IOP Conf. Series: Mat. Sci. and Eng.*, 346, 2018, 012086.
27. P.M Ajith, Birendra Kumar Barik, P. Sathiya and S. Aravindan, "Multiobjective optimization of friction welding of UNS S32205 duplex stainless steel," *Def. Tech*, vol. 11 (2), 2015, pp.157-165.
28. P.M Ajith, T.M. Afsal Husain, P. Sathiya and S. Aravindan, "Multi-objective optimization of continuous drive friction welding process parameters using response surface methodology with the intelligent optimization algorithm," *J. Iron and Ste. Res. Inter.*, vol. 22(10), 2015, pp.954-960.
29. S.S Kumaran, S. Muthukumaran and S. Vinodh, "Optimization of friction welding of tube to tube plate using an external tool by hybrid approach," *J. Alloys and Comp.*, vol. 509(6), 2011, pp. 2758–2769.
30. J. Leśniewski and A. Ambroziak, "Modelling the friction welding of titanium and tungsten pseudo-alloy," *Arch. Civil and Mech. Eng.*, vol. 15(1), 2015, pp. 142-150.
31. K Anand, Birendra Kumar Barik, K. Tamilmannan, P. Sathiya, "Artificial neural network modeling studies to predict the friction welding process parameters of Incoloy 800H joints," *Eng. Sci. and Tech.*, vol. 18 (3)3, 2015, pp. 394-407.
32. J.S.R Jang, "ANFIS: adaptive-network-based fuzzy inference system," *IEEE Trans. on Syst. Man and Cyber.*, vol. 23(3), 1993, pp. 665–685.
33. M.Vasudevan, K.N. Gowtham and T. Jayakumar, "Predicting depth of penetration, weld bead width and HAZ width in mod. 9Cr-1Mo steel welds using Adaptive Neuro Fuzzy Inference System (ANFIS) based models," *J. Comp. Mat. Sci. and Surf. Eng.*, vol. 4(3), 2011, pp. 205-218.
34. J.E. Raja Dhas and S. Kumanan, "ANFIS for prediction of weld bead width in a submerged arc welding process," *J. Sci. and Ind. Res.*, vol. 66, 2007, pp. 335–338.
35. Yulius Eka Agung Seputra and Bambang Soegijono, "Optimation of AMC's Tensile Properties Using

Adaptive Neuro-Fuzzy Inference System (ANFIS)," *IOP Conference Series: Mat. Sci. and Eng.*, 2019, 515, 012099.
36. Mohammad Ali Ansari and Reza Abdi Behnagh, "Numerical study of friction stir welding plunging phase using smoothed particle hydrodynamics," *Mod. and Sim. Mat. Sci. and Eng.*, vol. 27, 2019, 055006.
37. ASTM E8 / E8M-16a, Standard Test Methods for Tension Testing of Metallic Materials, ASTM International, West Conshohocken, PA,. https://www.astm.org › Standards & Publications.
38. Ranvijay Kumar, Rupinder Singh, I.P.S. Ahuja, Ada Amendola and Rosa Penna, "Friction welding for the manufacturing of PA6 and ABS structures reinforced with Fe particles," *Comp. Part B Eng.*, vol. 132, 2018, pp. 244-257.
39. K.N. Gowtham, M. Vasudevan, V. Maduraimuthu, T. Jayakumar, "Intelligent modeling combining Adaptive Neuro Fuzzy Inference System and Genetic Algorithm for optimizing welding process parameters," *Meta. and Mat. Trans.B*, vol. 42(2), 2011, pp. 385–392.

## AUTHORS PROFILE

**Dr.N.Mathiazhagan, PhD,** is a Professor in the department of Mechanical Engineering at Meenakshi Ramaswamy Engineering College, Ariyalur, Tamil Nadu, India. He has 18 years of teaching experience and 7 years of Industrial experience. After his Diploma degree in the year 1989, he received his Bachelor's Degree in 2003 from A.C.College of Engineering and Technology. His completed his M.E., in the year 2009 at Jayaram College of Engineering and Technology, Karattampatti. He completed his Ph.D at Anna University, Chennai, in the year 2017. He has the credit of publishing 29 International, 07 National and 4 national conference research articles. Composite Materials, Metal joining technology, Optimization and Characterization techniques are his areas of interest. He is a Life member of Indian Welding Society (IWS) and The Indian society for technical education (ISTE).

**I.Rajkumar, M.E.,** is an Assistant Professor in the Department of Mechanical Engineering at C.Abdul Hakeem College of Engineering & Technology, Melvisharam, Tamilnadu, India. He is a Post graduate in Manufacturing Engineering from Annamalai University (2004) and graduated at Amrita Insititute of Technology & Science (Presently Amrita Vishawa Vidhaya Peedam), Coimbatore as Production Engineer in the year 2002. He has 16 years of teaching experience and his areas of interest are Metal Joining, Composites and Optimization Techniques. He has published 02 International and 06 International conference articles. He is a life member of Indian Welding Society (IWS) and The Indian society for technical education (ISTE).